Downloaded from orbit.dtu.dk on: Apr 17, 2024

DTU Library

Bringing satellite winds to hub-height

Badger, Merete; Pena Diaz, Alfredo; Bredesen, Rolv Erlend; Berge, Erik; Hahmann, Andrea N.; Badger, Jake; Karagali, Ioanna; Hasager, Charlotte Bay; Mikkelsen, Torben

Published in:
Proceedings of EWEA 2012 - European Wind Energy Conference & Exhibition

Publication date:
2012

Document Version
Publisher's PDF, also known as Version of record

Link back to DTU Orbit

Citation (APA):
Badger, M., Pena Diaz, A., Bredesen, R. E., Berge, E., Hahmann, A. N., Badger, J., Karagali, I., Hasager, C. B., & Mikkelsen, T. (2012). Bringing satellite winds to hub-height. In *Proceedings of EWEA 2012 - European Wind Energy Conference & Exhibition* European Wind Energy Association (EWEA).

General rights
Copyright and moral rights for the publications made accessible in the public portal are retained by the authors and/or other copyright owners and it is a condition of accessing publications that users recognise and abide by the legal requirements associated with these rights.

- Users may download and print one copy of any publication from the public portal for the purpose of private study or research.
- You may not further distribute the material or use it for any profit-making activity or commercial gain
- You may freely distribute the URL identifying the publication in the public portal

If you believe that this document breaches copyright please contact us providing details, and we will remove access to the work immediately and investigate your claim.

Bringing satellite winds to hub-height

Merete Badger[1], Alfredo Peña[1], Rolv Erlend Bredesen[2], Erik Berge[2], Andrea Hahmann[1], Jake Badger[1], Ioanna Karagali[1], Charlotte Hasager[1], Torben Mikkelsen[1]

[1]DTU Wind Energy, Frederiksborgvej 399, 4000 Roskilde, Denmark
Corresponding author: Merete Badger, e-mail mebc@dtu.dk, phone +45 4677 5002

[2]Kjeller Vindteknikk, Gunnar Randers vei 12, Postboks 122, NO-2027 Kjeller, Norway

Summary

Satellite observations of the ocean surface can provide detailed information about the spatial wind variability over large areas. This is very valuable for the mapping of wind resources offshore where other measurements are costly and sparse. Satellite sensors operating at microwave frequencies measure the amount of radar backscatter from the sea surface, which is a function of the instant wind speed, wind direction, and satellite viewing geometry. A major limitation related to wind retrievals from satellite observations is that existing empirical model functions relate the radar backscatter to wind speed at the height 10 m only. The extrapolation of satellite wind fields to higher heights, which are more relevant for wind energy, remains a challenge which cannot be addressed by means of satellite data alone.

As part of the EU-NORSEWInD project (2008-12), a hybrid method has been developed, which combines the strengths of satellite winds and numerical modeling for offshore wind resource mapping. The vertical wind profile derived from numerical models is applied in order to bring the 10-m satellite winds and resource estimates up to turbine hub-height (~100 m). The method is tested over a focus area in the North Sea where offshore mast observations are also available. The 100-m wind resource maps based on satellite and model data agree very well. The results are promising for the future utilization of satellite observations in support of numerical model simulations for pre-feasibility studies.

1. Ocean winds from satellites

Mapping of ocean wind fields form space can be performed with two types of active microwave sensors: Scatterometers and synthetic aperture radar (SAR). Both types of satellite sensors orbit the Earth at an altitude of approximately 800 km, which is much closer than the geo-stationary satellites used for weather monitoring. The radar signal transmitted from space interacts with cm-scale waves at the sea surface, which are generated by the instant wind stress. The return signal is a function of these wind-generated waves and can thus be related to the wind speed.

Geophysical model functions (GMFs) are applied for the retrieval of ocean winds from satellite observations of radar backscatter [1,2]. The general form of these functions is:

$$\sigma^0 = U^{\gamma(\theta)} A(\theta) \left[1 + B(\theta,U)\cos\phi + C(\theta,U)\cos 2\phi\right] \quad (1)$$

where σ^0 is the normalized radar cross section (NRCS), U is wind speed at the height 10 m for a neutrally-stratified atmosphere, θ is the local incident angle, and ϕ is the wind direction with respect to the radar look direction. The coefficients A, B, C, and γ are functions of the wind speed and the local incident angle.

Some important characteristics of scatterometers and SAR sensors are given in Table 1. Their main difference, in connection with ocean wind retrievals, is that scatterometers provide daily global coverage whereas SAR acquisitions are more irregular and infrequent. The advantage of SAR is the much higher spatial resolution, which facilitates coverage of coastal seas.

Table 1. Characteristics of wind fields retrieved from scatterometer and C-band SAR sensors.

	Scatterometer	Synthetic Aperture Radar (SAR)
Retrieved parameters	Wind speed and direction	Wind speed
Spatial resolution	0.25° lat/lon	500 m
Spatial coverage	Global	Selected areas
Coastal mask	Up to 70 km from coastline	None
Temporal resolution	Twice daily	Variable – less than one per day
Temporal coverage	Systematically since 1991	ScanSAR since 1995
Current sensors	ASCAT, OSCAT, HY2A, MetOp-B	Envisat ASAR, Radarsat-1/2
Rain sensitivity	High – rain flags provided	Low

Scatterometers observe the sea surface from multiple angles at any given time. It is thus possible to retrieve both the wind speed and direction. The wind retrieval is typically performed by the data distributors. SAR sensors operate with a single antenna such that several wind speed and direction pairs correspond to a given NRCS. It is therefore necessary to obtain the wind direction from other sources before the wind speed can be retrieved. Wind retrievals from SAR are normally performed by the data users and it is common practice to use model wind directions as input to the GMF. SAR sensors operating at C-band (~5.3 GHz) are the most widely used for ocean wind retrievals.

2. From 10 m to hub-height

Satellite wind fields have previously been used for mapping of wind resources in the North Sea [3], Baltic Sea [4], and for projects in China, India, and the United Arab Emirates. The wind fields have also been used to study long-range wake effects of large offshore wind farms [5]. All of these analyses were restricted to the 10-m vertical level for which the satellite winds were retrieved. [6] lifted global scatterometer winds to the height 80 m and estimated the mean global wind power density. The accuracy of this estimate is unknown.

Here the possibility of combining the detailed spatial information from satellites with the vertical wind profiles of numerical models is investigated. [7] has developed a description of the vertical wind profile and validated it against mast and lidar data at high levels. This profile, which accounts for atmospheric stability effects and the atmospheric boundary-layer height, is used to bring 10-m satellite winds to the hub-height of modern wind turbines (100 m or higher). As part of the project EU-NORSEWInD, a large data base containing satellite data, model simulations, mast and lidar observations has been generated. This extensive collection of data is the starting point of our analysis.

3. Data

3.1 Satellite winds

The focus of this paper is on lifting of SAR wind fields but a similar approach can be taken for lifting of scatterometer wind fields. A data set of 80 Envisat ASAR scenes from the European

Space Agency is used. The scenes have been acquired during the one-year period covered by detailed numerical modeling over the North Sea (see 3.2). The 10-m wind fields have been retrieved by Collecte Localisation Satellites (CLS) in France (http://soprano.cls.fr).

3.2 Numerical modeling

Numerical modeling has been performed using the Weather Research and Forecasting Model (WRF) nested over a focus area in the North Sea with a cell size of 2 km by 2 km for the inner domain. The focus area covers the German Bight and the west coast of Denmark for the one year following 1st of May 2006. The meso-scale model WRF solves coupled equations for all important physical processes (such as winds, temperatures, stability, clouds, radiation etc.) in the atmosphere based on the initial fields and the lateral boundary values derived from global data. With the current setup, the WRF-model calculates the change in the meteorological fields for each grid-cell for a time step of 8 seconds. Thus a realistic temporal development of the meteorological variables is achieved. Data is stored to disk every 1 hours of simulation.

The parameterizations of to the vertical exchange of momentum and heat near the surface applied to the present runs are listed below. The particular parameter option number and name are also given.

Table 2 Selected WRF options for the vertical exchange (diffusion) of momentum and heat near the surface.

Option (name and value)	**Description**
Boundary layer option **(bl_pbl_physics=1)**	YSU–scheme in the planetary boundary (mixed) layer
Surface layer option **(sf_sfclay_physics=1)**	Monin Obukhov similarity in the constant flux layer
Land model option **(sf_surface_physics=1)**	Thermal diffusion scheme between land/sea and air

We refer to [8] for a detailed overview of the different physics options in WRF. The selected parameterization (YSU-scheme) is additionally described in [9-11]. A comparison of how the YSU-scheme performs over land at the Danish site Høvsøre for October 2009 against other PBL-schemes is found in [12].

3.3 Mast observations

Wind speed observations from the German mast Fino-1 (6.59°E, 54.01°N) are used for validation of the 100-m wind speed estimates from SAR and WRF. The measurements at 100 m are obtained at the top of the mast where the flow conditions are somewhat different from the lower measurement levels. The effect of flow distortion should be limited at 100 m compared to the lower levels where mast effects are evident. However, some flow distortion may still occur at 100 m.

4. Methodology

The first step in our analysis is to derive the friction velocity, u_* from the 10-m wind from SAR. Eq. 2, which describes the logarithmic wind profile for neutral conditions, is combined with Eq. 3, Charnock's equation. Then u_{*SAR} is estimated through iteration:

$$u_{10SAR} = \frac{u_{*SAR}}{\kappa}\left[\ln\frac{10}{z_0}\right] \qquad (2)$$

$$z_0 = \alpha_c \frac{u_*^2}{g} \qquad (3)$$

where κ is von Karman's constant of 0.4, z_0 is the aerodynamic roughness length, g is the acceleration due to gravity, and α_c is Charnock's parameter of 0.0144.

The second step is to estimate the atmospheric stability expressed as the Obukhov length, L from Eq. 4. Stable conditions occur for $L>0$ and unstable conditions occur for $L\leq 0$. Inputs are u_{*SAR} and the WRF parameters $T2$ and HFX, which give the air temperature and heat flux.

$$L_{WRF/SAR} = \frac{-u_{*SAR}^3 \, T2_{WRF}}{g \, \kappa \, HFX_{WRF}} \tag{4}$$

Eq. 5-7 are applied to calculate the stability function, ψ_m for a given height; here the height 100 m is chosen:

$L>0$: $$\psi_m = -4.7 \frac{z}{L_{WRF/SAR}} \tag{5}$$

$L\leq 0$: $$\psi_m = \frac{3}{2} \ln\left(\frac{1+x+x^2}{3}\right) - \sqrt{3} \arctan\left(\frac{2x+1}{\sqrt{3}}\right) + \frac{\pi}{\sqrt{3}} \tag{6}$$

$$x = \left(1 - 12 \frac{z}{L_{WRF/SAR}}\right)^{1/3} \tag{7}$$

Finally, the wind speed at 100 m, u_{100SAR} is estimated from Eq. 8 and 9 using, for stable conditions, the WRF parameter $PBLH$ to describe the planetary boundary-layer height.

$L_{WRF/SAR}>0$: $$u_{100\,SAR} = \frac{u_{*SAR}}{\kappa} \left[\ln \frac{100}{z_0} - \psi_{\left(\frac{100}{L_{WRF/SAR}}\right)} \left(1 - \frac{100}{2PBLH}\right) \right] \tag{8}$$

$L_{WRF/SAR}\leq 0$: $$u_{100\,SAR} = \frac{u_{*SAR}}{\kappa} \left[\ln \frac{100}{z_0} - \psi_{\left(\frac{100}{L_{WRF/SAR}}\right)} \right] \tag{9}$$

In practical terms, the ratio of wind speeds between 100 m and 10 m is calculated. This lifting coefficient is then applied to lift the 10-m satellite winds.

5. Results

At Fino-1, a concurrent comparison of lifted SAR and WRF wind speeds against measurements at 100 m give the statistics presented in Table 3 and Figure 1. The results show that the SAR winds at 100 m are on average significantly lower than the winds measured at the Fino-1 platform. The WRF winds are also lower than the mast observations but closer than the SAR data.

Table 3. Mean wind speed, RMS error, and bias for different wind speed data at Fino-1, 100 m. The RMS error and bias is given for (SAR-mast) and (WRF-mast) using only WRF samples concurrent with the SAR samples.

	U (m/s)	RMS error (m/s)	Bias (m/s)
Mast	10.74	-	-
SAR	9.77	2.22	-0.97
WRF	10.46	1.75	-0.27

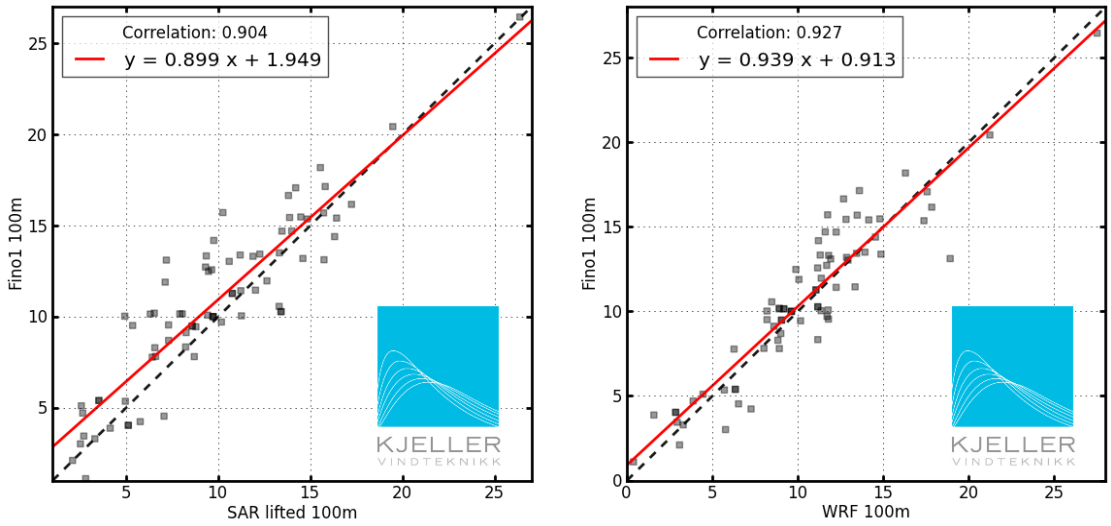

Figure 1. Plots of (left) lifted SAR wind speeds and (right) WRF wind speeds against observations at Fino-1 at 100 m. All in m/s.

Figure 2 shows the frequency distributions of winds at Fino-1 from mast, lifted SAR, and WRF data together with the Weibull functions fitted to each data set. The Weibull parameters from the satellite data deviate from the other two data sets as it is expected from the difference in mean wind speeds described above. All of the plots lack the smooth appearance which is normally seen from frequency plots of time series observations. This is due to the very limited number of samples investigated here (80 satellite SAR scenes).

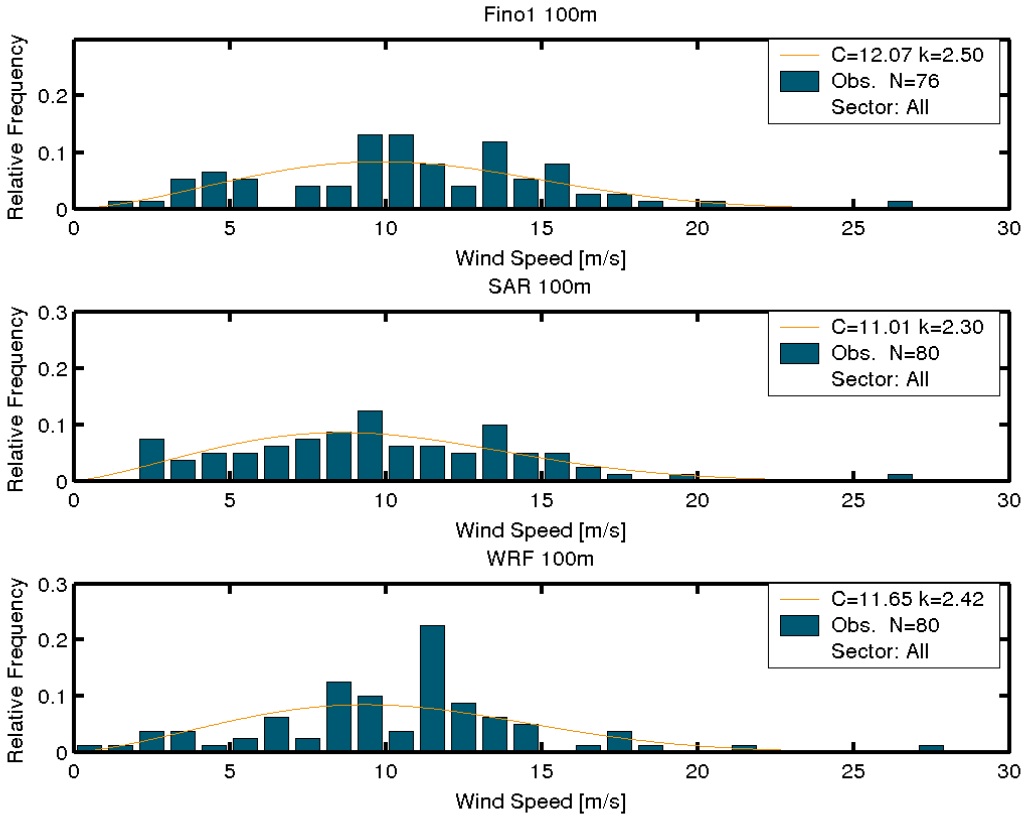

Figure 2. Frequency distribution of winds at Fino-1, 100 m based on (upper) mast observations, (middle) lifted SAR winds, and (lower) WRF winds.

The spatial distribution of the lifted average SAR wind speed is shown in Figure 3 (left). The linear features are artifacts caused by the edges of individual satellite scenes. If these contours are neglected, the spatial variability of the mean wind speed from SAR is similar to that of WRF simulations. This is also seen from the map of mean differences between concurrent SAR and WRF wind speeds in Figure 3 (right). The mean differences are negative all over the North Sea but with very small values in the northern part of the map. Differences between the two wind data sets increase towards the south and become as high as -3 m/s near the coastlines of Germany and the Netherlands. This suggests that the relatively large negative biases found for SAR winds at Fino-1 are not representative for the entire study area.

Figure 4 shows the effect of a limited number of samples, which can be achieved from satellite SAR, illustrated with the WRF data set. The map to the left shows the mean wind speed from the full WRF data set with hourly simulations over one year. The map to the right shows differences in mean wind speed between the WRF simulations concurrent with SAR data acquisitions and the full WRF data set. The map suggests that the consequence of the limited number of samples is mostly a negative bias. The difference between the two data sets can be as high as -0.8 m/s but for most parts of the study area the difference is smaller.

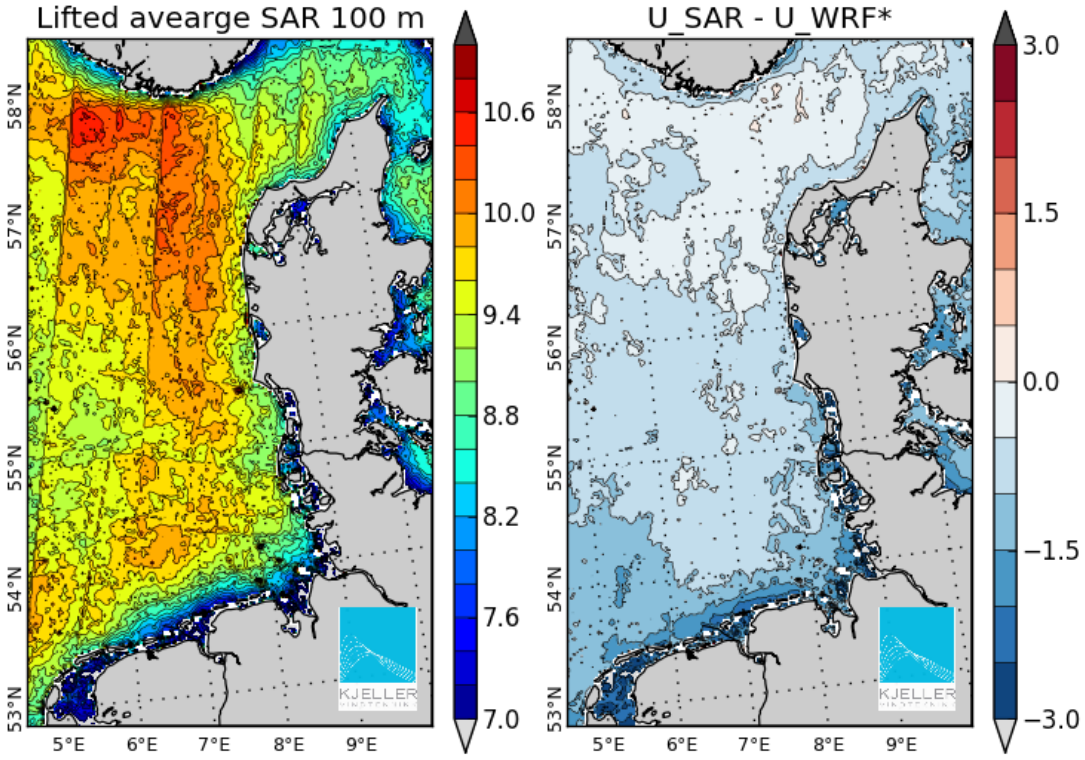

Figure 3. Left: mean wind speed (m/s) from a total of 80 SAR scenes lifted to 100 m. Right: Plot of the difference between 100-m SAR and WRF wind speeds (m/s) where U_WRF indicates WRF simulations concurrent with the SAR data acquisitions.*

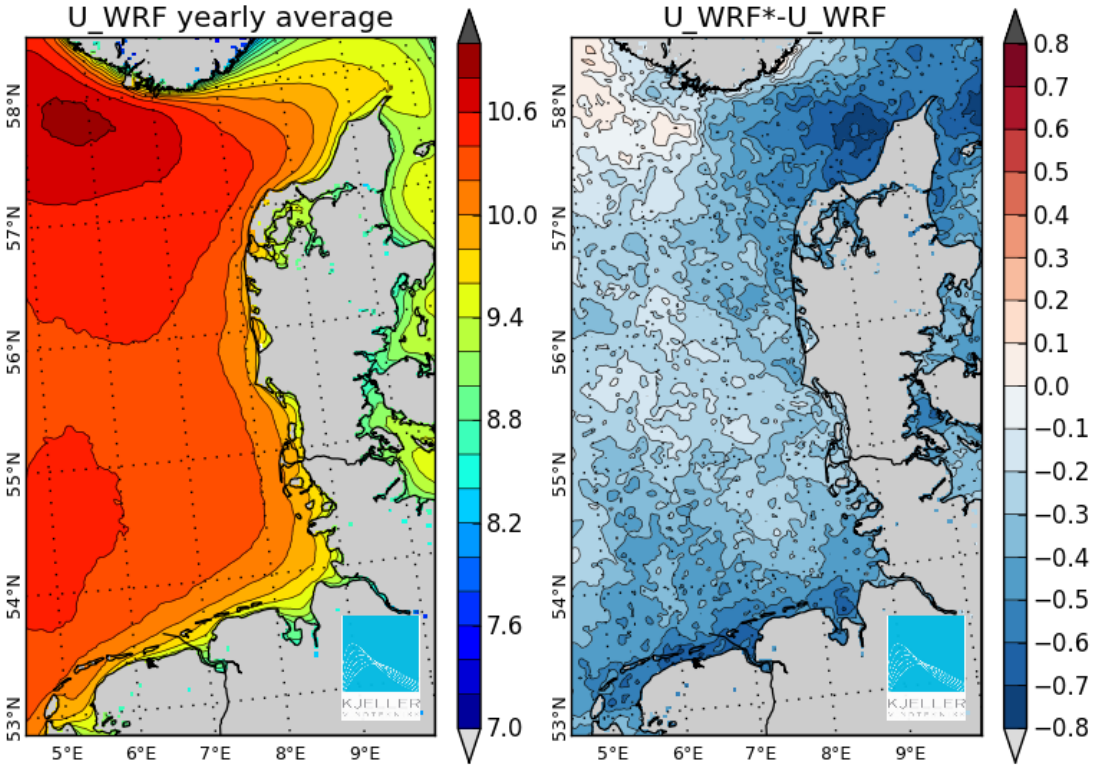

Figure 4. Left: Mean wind speed (m/s) at 100 m from one year of hourly WRF simulations. Right: Differences between the mean wind speed (m/s) from the 80 WRF simulations concurrent with SAR data acquisitions (U_WRF) and the full WRF data set (U_WRF).*

6. Discussion

Over most parts of the North Sea, mean differences between 100-m winds from satellite SAR and numerical modeling do not exceed -1 m/s. The larger negative bias found at Fino-1, also with respect to mast observations, is therefore not representative for the entire North Sea. Previous comparisons between SAR and mast wind speeds at 10 m have also revealed a negative bias of the SAR winds [4,13]. The bias and RMS error found in this analysis are larger than for the previous studies and there are several possible reasons for this:

The impact of atmospheric stability effects on the wind speed is much larger when wind speed data are lifted from 10 m to 100 m compared to a situation where 10-m SAR winds are compared to measurements at lower levels. The errors introduced in the lifting procedure depend on the accuracy of the wind profile description and, in our case, the WRF parameters used as input to the lifting equations. The wind profile description used in this study has been validated for a site in the North Sea and for high vertical levels. It is therefore expected to give a more accurate wind speed at 100 m than other descriptions of the vertical wind profile.

The WRF parameters used in this study are known to describe the average meteorological conditions over long periods well [14]. For instant weather situations, like the situations captured by satellite SAR snapshots, the accuracy of $T2$, HFX, and $PBLH$ is questionable. It depends to a large degree on the accuracy of inputs used for the WRF simulation; especially for the sea surface temperature, SST. The large differences between SAR and WRF winds near the coast of Germany and the Netherlands may be a consequence of the diffusive nature of WRF.

The choice of GMF used for the SAR wind retrieval will impact the accuracy. Several different GMF's are available and so far, the performance of these GMF's has not been compared systematically against a single ground truth data set. The accuracy of mast measurements at Fino-1 and effects of flow distortion at different levels is unknown. Differences between the wind speed data sets may thus originate partly from errors in the measured winds. Finally, the data set analyzed here is small and the most extreme differences between the different data sets will therefore have a large impact on the mean values.

7. Conclusion

The analysis presented here shows that satellite winds retrieved for the height 10 m can be lifted to 100 m and beyond using data from numerical models to describe the atmospheric stability and the boundary-layer height. These two parameters are essential for an accurate estimation of wind profiles at high vertical levels. Work is in progress to analyze additional stations where measurements are available and also to extend the period covered by detailed model simulations such that a larger data set of concurrent SAR-WRF samples can be obtained. A reliable method for lifting of satellite winds has a large potential for wind energy applications, as the winds can be used directly for wind resource assessment and wake analyses at the wind turbine hub height.

Acknowledgements

The work was funded through the project EU-NORSEWInD (TREN-FP7EN-21908). Satellite data from the European Space Agency are acknowledged. Collecte Localisation Satellites (CLS) is thanked for the SAR wind retrievals. Fino-1 data were provided by Bundesministerium für Umwelt (BMU), Projektträger Juelich (PTJ), Deutsches Windenergie Institut (DEWI).

References

1. Hersbach H, Stoffelen A, de Haan S. An Improved C-band Scatterometer Ocean Geophysical Model Function: CMOD5. *J. Geophys. Res.* 2007; 112*,* C03006, doi: 10.1029/2006JC003743, 2007.

2. Hersbach H. Comparison of C-band Scatterometer CMOD5.N Equivalent Neutral Winds with ECMWF. *J. Atmos. Oceanic Technol. 2010; 27:*721-736.

3. Badger M, Badger J, Nielsen M, Hasager CB, Peña A. Wind class sampling of satellite SAR imagery for offshore wind resource mapping. *Journal of Applied Meteorology and Climatology* 2010; 49:2474-2491.

4. Hasager CB, Badger M, Peña A, Larsén XG, Bingöl F. SAR-based Wind Resource Statistics in the Baltic Sea. *Remote Sensing* 2011; 3:117-144.

5. Christiansen MB, Hasager CB. Wake effects of large offshore wind farms identified from satellite SAR. *Remote Sensing of Environment* 2005; 98:251-268.

6. Capps SB, Zender CS. Global wind power sensitivity to surface layer stability. *Geophysical Research Letters* 2009; 36, L09801, doi: 10.1029/2008GL037063.

7. Peña A, Gryning S-E, Hasager CB. Measurements and Modelling of the Wind Speed Profile in the Marine Atmospheric Boundary Layer. *Bound.-Layer Meteor.* 2008; 129:479-495.

8. Skamarock WC, Klemp JB, Dudhia J, Gill DO,. Barker DM, Duda MG, et al. *A Description of the Advanced Research WRF Version 3:* NCAR: Boulder, U.S., 2008.

9. Hong S, Noh Y. Nonlocal boundary layer vertical diffusion in a medium-range forest model. *Monthly Weather Review* 1996;124:2322-2339.

10. Hong S, Noh Y, Dudhia J. A new vertical diffusin package with an explicit treatment of entrainment processes. *Monthly Weather Review* 2006; 134:2318- 2341.

11. Hong S, Kim S. Stable Boundary Layer Mixing in a Vertical Diffusion Scheme. *18th Symposium on Boundary Layers and Turbulence,* 2008.

12. Draxl C, Hahmann AN, Peña A, Nissen JN, Giebel G. Validation of boundary-layer winds from WRF mesoscale forecasts with applications to wind energy forecasting. *19th Symposium on Boundary Layers and Turbulence* 2010.

13. Christiansen MB, Koch W, Horstmann J, Hasager CB, Nielsen M. Wind resource assessment from C-band SAR. *Remote Sensing of Environment 2006;* 105:68-81.

14. Peña A, Hahmann AN. Atmospheric stability and turbulence fluxes at Horns Rev—an intercomparison of sonic, bulk and WRF model data, *Wind Energy* in press; doi: 10.1002/we.500.